

University of Natural Resources and Life Sciences Vienna



Department of Biotechnology  
Extremophile Center

Transcriptome Analysis of  
*Cladophialophora immunda*  
using toluene as carbon source

Masterthesis

submitted by  
Christina Kustor, BSc.  
Vienna, 2016

Supervisor: Katja Sterflinger-Gleixner, Assoc. Prof. Dr.  
Co-Supervisor: Hakim Tafer, Dr.

## Acknowledgement

# Abstract

The extremophilic fungi *Cladophialophora immunda* is known for the capability to grow on aromatic hydrocarbons and moreover for the ability to degrade hydrocarbons.

The thesis analyse transcriptomes of *Cladophialophora immunda* and which genes are transcribed under different conditions. The transcriptome data were obtained with RNA sequencing and the analysis were realised with bioinformatics methods. A workflow system for genome annotation with RNA sequencing data was developed and followed by performing statistics to obtain a list of genes and their expression level differences between two groups. Furthermore functional annotation and additional enrichment analysis were performed.

Many biological processes regarding to energy generation are down-regulated. Whereas genes coding for specific protein metabolic processes and protein folding are highly expressed. The genes coding enzymes for toluene degradation are up-regulated too. This could be the reason that cells can survive in such extreme environments.

**Keywords:** Extremophilic fungi, black yeasts, transcriptome analysis, toluene degradation,

# Zusammenfassung

Der extremophile Pilz *Cladophialophora immunda* ist bekannt für seine Fähigkeit auf aromatischen Kohlenwasserstoffen zu wachsen und noch viel mehr für seine Fähigkeit Kohlenwasserstoffe abzubauen.

Diese Masterarbeit analysiert die Transkriptome von *Cladophialophora immunda* und welche Gene unter verschiedenene Bediengungen transkribiert werden. Die Transkriptomdaten wurden durch RNA Sequenzierung erhalten und mit bioinformatischen Methoden analysiert.

Es wurde ein Workflow System für Genomannotierung mit RNA-Sequenzierdaten entwickelt und anschließend die Statistik durchgeführt, um eine Liste mit Genen und deren Unterschiede der Expressionshöhe zwischen zwei Gruppen zu ermitteln. Weiters wurde funktionelle Annotierung und die dazugehörigen Enrichment Analysen realisiert.

Viele biologische Prozesse bezüglich Energieerzeugung sind runter reguliert. Wohingegen Gene, die für spezifische metabolische Proteinprozesse und Proteinfaltung codieren, höher exprimiert sind. Die Gene, die Enzyme für den Toluennabbau codieren, sind ebenfalls hoch reguliert. Das kann die Ursache sein, warum Zellen in solchen extremen Umgebungen überleben können.

**Stichwörter:** Extremophile Pilze, schwarze Hefen, Transkriptomanalysen, Toluennabbau

# Contents

<b>Introduction</b>	<b>5</b>
1.1 Extremophilic fungi . . . . .	5
1.2 Black yeasts . . . . .	5
1.3 Bioremediation . . . . .	6
1.4 Study of <i>Cladophialophora immunda</i> . . . . .	8
1.5 Transcriptome Analysis . . . . .	10
1.5.1 RNA sequencing . . . . .	10
1.6 Bioinformatics methods . . . . .	11
1.6.1 Workflow System . . . . .	11
<b>Methods</b>	<b>13</b>
2.1 Growth of <i>Cladophialophora immunda</i> . . . . .	13
2.2 RNA-seq library preparation . . . . .	14
2.3 Mapping Algorithm . . . . .	14
2.3.1 Suffix Tree . . . . .	15
2.3.2 <i>STAR</i> specific approach . . . . .	15
2.4 Count Algorithm . . . . .	16
2.5 Differential Expression Algorithm . . . . .	17
2.6 Enrichment Approach . . . . .	19
2.7 Pipeline implementation . . . . .	20
<b>Results</b>	<b>27</b>
3.1 Up- and Down-regulated genes . . . . .	27
3.2 Functional enrichment . . . . .	30
3.2.1 Gene Ontology . . . . .	30

3.2.2	KEGG . . . . .	34
3.2.3	Differentially expressed proteins . . . . .	35
3.3	Toluene Degradation . . . . .	37
	<b>Discussion</b>	<b>39</b>
	<b>Conclusion</b>	<b>40</b>
	<b>Bibliography</b>	<b>46</b>
	<b>List of Figures</b>	<b>47</b>
	<b>List of Tables</b>	<b>48</b>

# Introduction

## 1.1 Extremophilic fungi

An extremophile is an organism that thrives in an extreme environment. The habitants are quite different including the physical extremes for instance temperature, UV radiation or pressure and the geochemical extremes such as desiccation, salinity, pH or redox potential. [26] In the last decade the interest of extreme environments and the previously unknown extremophilic microorganisms in such region has increased. The enthusiasm to isolate them in pure culture and profile their metabolites make them so attractive for research. Their products have potential to be valuable resources for the development of a bio-based economy through their application to different branches in biotechnology. [24]

The diversity of fungi to occur in stressful environments that are hostile to most eukaryotes is one of the greatest in microorganisms. Comparative results of evolutionary studies have attempted to explain adaptability of extremophiles. Fungi from extremely cold and salty habitats share patterns in morphology, phylogeny and population. [6]

## 1.2 Black yeasts

"Black yeasts" is a *terminus technicus* subscribing a group of fungi that conquer extreme environments characterized by oligotrophic nutrient conditions, elevated temperatures, UV radiation, matrix and osmotic stress and combinations of these factors. Other terms are "meristematic fungi" and "MCF" Meristematic fungi was first mentioned by de Hoog and Hermanides Nijhof in 1977, for fungi that form

aggregates of thick-walled, melanized cells enlarging and reproducing by isodiametrical division. MCF refers to growth pattern of meristematic fungi and some black yeasts. These fungi grow in mineral substrates like rock but also glass or metal.[30]

The combined influence of the mentioned stress factors exerts a high selective pressure on the microbial community and as a consequence black yeasts are rarely found in complex microbial populations. Black yeasts are quite heterogeneous from taxonomic and phylogenetic point of view but they have in common melanized cell walls. The production of melanins and the incrustation of the cell walls with this high-molecular substances are the most important factors in stress resistance of black yeasts. The black yeasts include species are also found in human environments and have a human-pathogenic potential. Beside the protection factor, melanin also affect the penetration of host tissue in plants, animal and human tissue. *Exophiala dermatitidis* and *Cryptococcus neoformans* are such human pathogenic yeasts where melanin is one of the virulence factors. [11, 30] Other black fungi that associated with humans are represented by the typical black yeasts belonging to the genera *Fonsecaea*, *Capronia*, *Phaeococcomyces* and *Cladophialophora*. [4]

The group of black fungi was chosen for the purpose of bioremediation, as they are found in extreme environments and therefore resistant to stress conditions. [22]

### 1.3 Bioremediation

Toluene and other related aromatic hydrocarbons are abundant environmental pollutants. Bioremediation of pollutants is an attractive method because of its environmental and economical advantages. The use of bacteria for biodegradation of toluene to CO<sub>2</sub>, water and biomass has been studied widely. However the benefit of fungi for this purpose becomes very important, chiefly because of the advantages under conditions of reduced water activity and low pH, which often prevail in biofilters. [18] The process of using fungi to degrade contaminants in the environment is also termed mycoremediation. This biological treatment can be differentiated into bio-augmentation, biosparging, bioventing, composting and several other less frequently applied methods. The method of the preceding study was bioaug-

mentation, a bioremediation option for hydrocarbon-contaminated, oily-sludge restoration. Bioavailability of the contaminant for the microorganisms, the degradation to less toxic compounds and the opportunity for optimization of biological activity are critical points in bioremediation. [22]

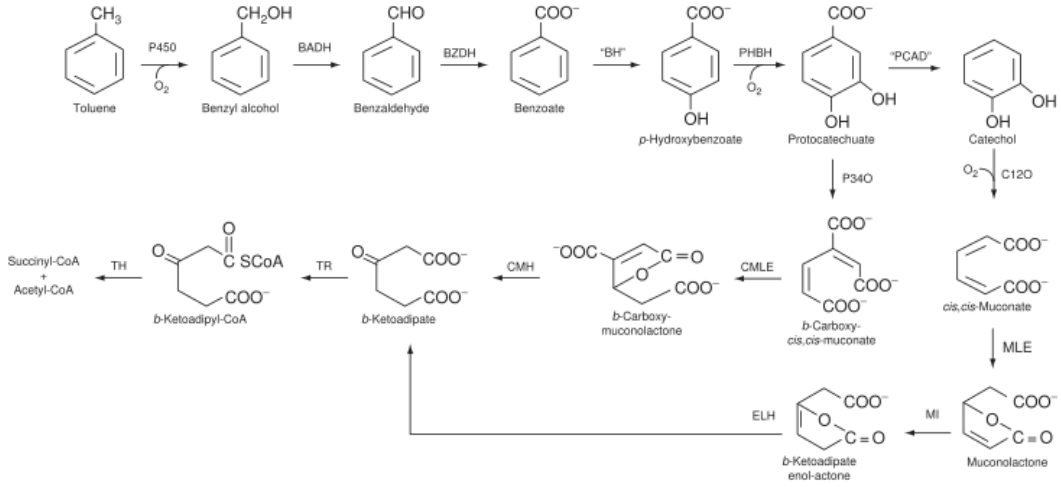


Figure 1: Toluene degradation pathway

Toluene (methylbenzene) is an aromatic hydrocarbon natural product of diagenic origin and an important commercial chemical. The BTEX mixtures referred to in bioremediation applications contain benzene, ethylbenzene, toluene and xylenes. These toxic compounds are usually difficult to remove to their wide dispersal in ecosystem.

A toluene degradation pathway in fungi was first proposed for *Cladophialophora saturnica* [2] and in an other previous study the connection between toluene metabolism and cytochrome P450 was established [18]. The examinations for this presence of genes belonging to the pathway for the toluene degradation (figure 1) were done in comparison with the genome of the model yeast *Saccharomyces cerevisiae*. [3]

## 1.4 Study of *Cladophialophora immunda*

The black yeast *Cladophialophora immunda* is known for the capability to grow on aromatic hydrocarbons and moreover for the ability to degrade hydrocarbons. The genus *Cladophialophora* belongs to the ascomycetes and forms two phylogenetic glades (*Carrionii* and *Bantiana*) in the family of *Herpotrichiellaceae*, order *Chaetothyriales*. *Cladophialophora* is morphologically characterized by one-celled, ellipsoidal to fusiform, dry conidia arising through blastic, acropetal conidiogenesis and arranged in branched chains. The genus includes species causing skin infections and other human diseases. *C. immunda* is of special medical and biotechnological interest because it is frequently isolated both from humans and from contaminated soil. [31, 2]

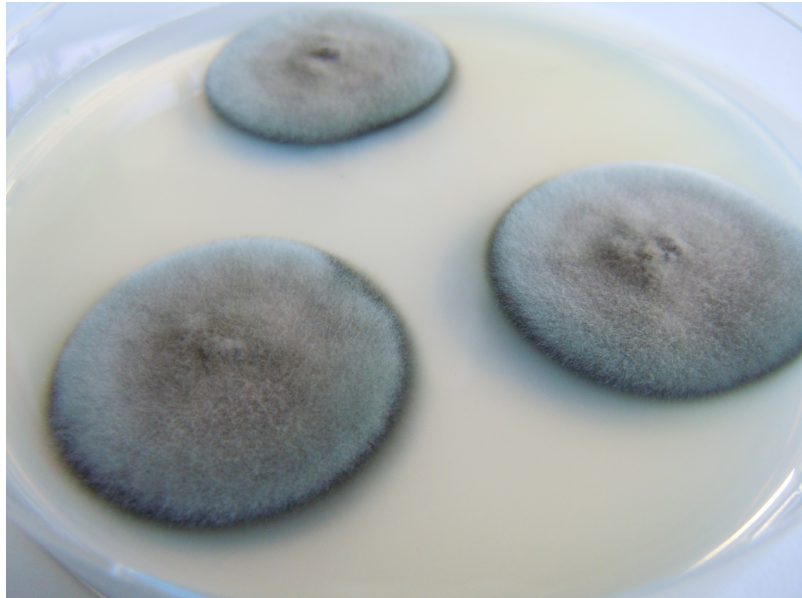


Figure 2: *Cladophialophora immunda*

*Cladophialophora immunda* was isolated from a gasoline station, in a hydrocarbon rich environment, therefore the fungi is an important candidate for bioremediation and for application in biofilters. [23]

To better understand the mechanisms of black yeasts and their effect to degrade hydrocarbons, a preceding study on bioremediation was done. Therefore a collection

of 163 strains of black yeast-like fungi from the CBS Fungal Biodiversity Center (Utrecht, The Netherlands) has been screened for the ability to grow on hexadecane, toluene and polychlorinated biphenyl 126 (PCB126) as the sole carbon and energy source. These compounds were chosen as representatives of relevant environmental pollutants. The results indicated that the two strains of *C. immunda* and *Exophiala mesophila* are able to grow on media with toluene as carbon source, confirmed by an increase in CO<sub>2</sub> and a toluene decrease shown in figure 3. [3, 22]

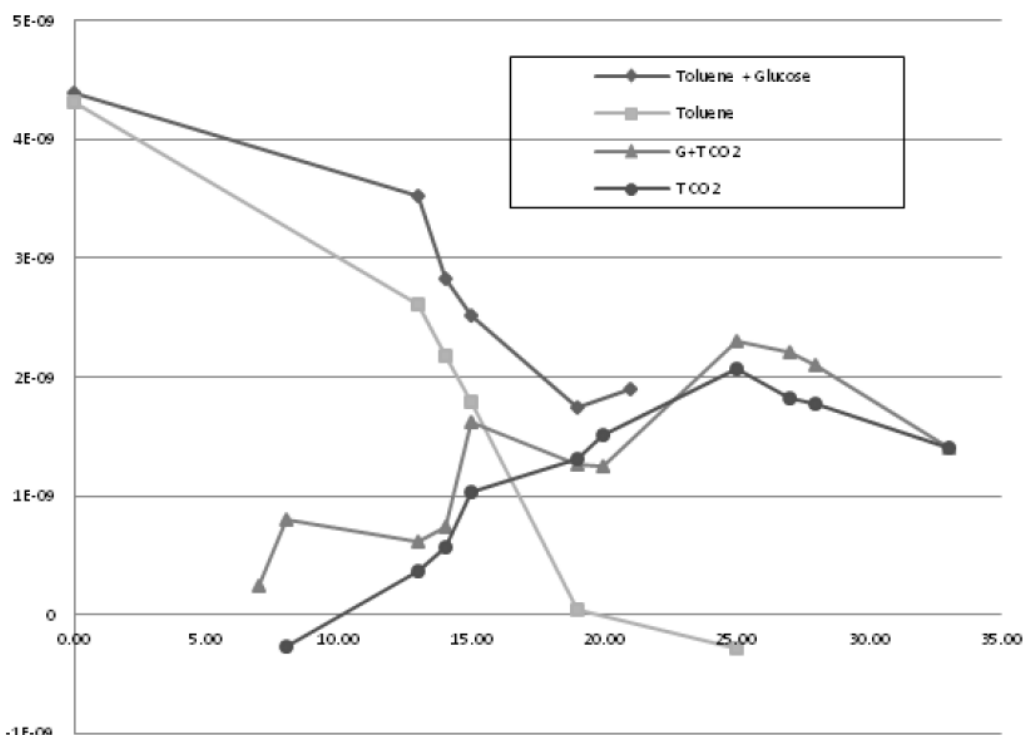


Figure 3: Toluene and CO<sub>2</sub> values for *C. immunda*: Carbon equivalence [mol] of the two molecules was plotted against runtime [days]. [22]

Together all the recent studies indicate that maybe the analysis of transcriptome will answer all the question about that special fungi. Accordingly the aim of the thesis is to examine the way in which the transcriptomes of *Cladophialophora immunda* can be determined and identify which genes are transcribed under different conditions. The major issue is to determine the pathways that allow *C. immunda* to use toluene as carbon source.

The transcriptome data were obtained with RNA-seq performed by Ion Torrent technology coupled with the Ion Proton sequencer (Life Technologies, Carlsbad, CA). [3]

## 1.5 Transcriptome Analysis

The powerful technology RNA-sequencing and the analysis of transcriptomes, to know which gene is expressed, became an important method in science. Transcriptome analysis enables the understanding of how sets of genes work together to form metabolic, regulatory and signalling pathways within a cell. [35]

### 1.5.1 RNA sequencing

RNAs in total or fractioned are first converted into a library of cDNA fragments. Sequencing adaptors are added to each cDNA fragment to one or both ends. Each molecule is then sequenced in a high-throughput manner to obtain short sequences from one end (single-end sequencing) or both ends (pair-end sequencing). The reads are typically 30–400 bp, depending on the sequencing technology used. If the resulting sequence reads have been obtained, the first task of data analysis is to map the short reads from RNA-seq to the reference genome or to assemble them into contigs before aligning them to the genomic sequence to reveal transcription structure. The way of analysing transcriptomic data differs considering short reads also contain reads that span exon junctions or that contain poly(A) ends. Alignment can be also complicated for large transcriptomes as a result of matching multiple locations in the genome with a significant portion of sequence reads. [34]

An advantage of RNA-seq from earlier methods, such as microarrays, is the high throughput of current RNA-seq platforms, the sensitivity afforded by newer technologies and the ability to discover novel transcripts, gene models and non-coding RNA species. [13]

## 1.6 Bioinformatics methods

The increasing use of next-generation sequencing methods is related to a large amount of produced data, which has to be analysed and interpreted. Therefore bioinformatics methods are a necessary step in analysing transcriptomes. As RNA-seq is an active field of research producing new approaches and tools at a rapid pace, many alternative programs exist for each analysis step. [13]

### 1.6.1 Workflow System

The data analysing steps were performed by different programs and tools, which may need specific data formats and external files. The multiple steps can be handled through scripting a reusable pipeline with defined inputs, outputs and parameters for each step.

The software Snakemake was used to evolve the pipelines for genome annotation, functional annotation and enrichment analysis. Snakemake is based in Python language and can be used on a single core workstation as well as on a cluster without modifying the workflow. Snakemake's option "-dag" creates the directed acyclic graph (DAG) of executed jobs. [14]

In figure 4 exemplified the DAG of the educed Snakemake file. Jobs (i.e. the execution of a rule) are depicted as nodes, a directed edge between two jobs means that the rule underlying the second job needs the output of the job executed before as an input file. A path represents a sequence of jobs that have to be executed serially.



Figure 4: Directed acyclic graph (DAG) of a Snakemakefile

# Methods

## 2.1 Growth of *Cladophialophora immunda*

For the experimental conditions, the cultivation of *Cladophialophora immunda* with glucose or toluene as carbon-source was chosen.

The *Cladophialophora immunda* strain (CBS 110551) was isolated from a toluene-charged air biofilter inoculated with gasoline-polluted soil. [23]

*Cladophialophora immunda* (CBS 110551) was cultured in malt extract agarose media (2 % malt extract, 2 % D-glucose, 0.1 % bacto-peptone and 2 % agar).

For the RNA-seq experiments, *C. immunda* was grown in liquid culture in a modified Hartmans' mineral media with 2 % glucose or 1.35 mM toluene as carbon sources. [10] The toluene was supplied through the air of a sealed flask in a 5 % solution in dibutylphthalate. The experiments duration was 90 days (growth with toluene) and one week (growth with glucose) at the temperature of 22 °C at 100 rpm on an orbital shaker. Both experiments were performed in 3 biological replicates. At the end of the experiments the biomass was collected by centrifugation (5000 g per 15 minutes at 4 °C), washed with RNase free water, frozen in liquid nitrogen and stored at -80 °C until use.

The medium (1 litre of demineralized water) is composed by:

Solution A: 10 mL

Solution B: 25 mL

+ 0.02 % yeast extract as nitrogen source

Solution A (1 litre demineralized water)		Solution B (1 litre demineralized water)	
$(\text{NH}_4)_2\text{SO}_4$	200 g	$\text{K}_2\text{HPO}_4$	155 g
$\text{MgCl}_2 \cdot 6\text{H}_2\text{O}$	10 g	$\text{NaH}_2\text{PO}_4 \cdot 2\text{H}_2\text{O}$	85 g
EDTA	1 g		
$\text{ZnSO}_4 \cdot 7\text{H}_2\text{O}$	0.2g		
$\text{CaCl}_2 \cdot 2\text{H}_2\text{O}$	0.1 g		
$\text{FeSO}_4 \cdot 7\text{H}_2\text{O}$	0.5 g		
$\text{Na}_2\text{MoO}_4 \cdot 2\text{H}_2\text{O}$	0.02 g		
$\text{CuSO}_4 \cdot 5\text{H}_2\text{O}$	0.02 g		
$\text{CoCl}_2 \cdot 6\text{H}_2\text{O}$	0.04 g		
$\text{MnCl}_2 \cdot 2\text{H}_2\text{O}$	0.1 g		

Table 1: Hartmans'mineral media

## 2.2 RNA-seq library preparation

The work in the laboratory included the extraction of total RNA from 100 mg of fungal biomass with FastRNA PRO™ RED KIT (MP Biomedicals) according to the instructions of the manufacturer. The mRNA was isolated with the Dynabeads® mRNA DIRECT™ Micro Kit (Ambion by Life Technologies) and the following transcriptome library preparation was performed with the Ion Total RNA-Seq Kit v2 (Life Technologies). Total RNA, isolated mRNA and the final cDNA library were all qualitatively and quantitatively evaluated by mean of Agilent 2100 Bio-analyzer (Agilent Technologies, Santa Clara, CA). The RNA-seq was performed by the Ion Proton™ sequencer (Life Technologies) with the Ion PI Chip v2 (Life Technologies). The average read length of the six cDNA libraries was 175 bp for all five samples. Total reads generated per sample varied between 57,611,573 and 99,965,344.

## 2.3 Mapping Algorithm

The first step to understanding a genome structure is through genome mapping, which is a process of identifying relative locations of genes on a chromosome. When a read is mapped to reference genome, a sequence alignment is created. [35] The

input files in this case were the preprocessed reads and in addition the reference sequence.

### 2.3.1 Suffix Tree

The rapid advance of new sequencing technology expand the scale and resolution of many biological applications like quantitative analysis of transcriptome where sequence reads must be compared to a reference. There are different algorithms developed in the last few years. Some of them are based on hash tables and the others are based on suffix trees. The algorithm associates two steps, identifying exact matches and building inexact alignments supported by exact matches. Finding exact matches rely on a representation of suffix tree. The advantage in comparison to a hash table is that by using a tree the alignment to multiple identical copies of substring in the reference has to be done only once. Because the identical copies collapse on a single path in the tree, otherwise in a hash table index an alignment must be performed for each copy. [15]

A suffix tree is a data structure that stores all the suffixes of a string to enabling fast string matching. The time complexity of determining if a query has an exact match against a tree is linear in the length of the query, independent of the length of the reference sequence. Nonetheless a tree takes  $O(L^2)$  space, where  $L$  is the length of reference. To reduce the space a approach to achieves linear space while allowing linear time searching is used. In theory it is possible to represent a suffix tree  $L \log_2 L + O(L)$  bits using rank-selection operations. To solve this space efficient implementation, an enhanced suffix array was derived that consists of a suffix array and several auxiliary arrays. A suffix array can be regarded as an implicit representation of suffix tree and has an identical time complexity to suffix tree in finding exact matches. [15]

### 2.3.2 *STAR* specific approach

Mapping is computationally intensive, that is why the program *STAR* was chosen. *STAR* (Spliced Transcripts Alignment to a Reference) is a spliced alignment program which runs very fast. The benefits of *STAR* are largely based on the

Maximum Mappable Length approach.

The algorithm Maximum Mappable Length (*MML*) was developed to align reads to the genome. The idea of *MML* approach is to search a Maximum Mappable Prefix (*MMP*). Given a read sequence  $R$ , read location  $i$  and a reference genome sequence  $G$ , the  $MMP(R, i, G)$  is defined as the longest substring

$$[R_i, R_{i+1}, \dots, R_{i+MML-1}]$$

which matches exactly one or more substrings of  $G$ , where *MML* is the maximum mappable length. Starting from the first base of the read the algorithm finds the *MMP*. If *MMP* can not be mapped contiguously to the genome because of an splice junction, this first seed will be mapped to a donor splice site. The *MMP* search is repeated for the unmapped portion of the read, which will be mapped to an acceptor splice site. The difference to other algorithm is to align the non-contiguous sequences directly to the reference genome, which accelerated the process to map. [5]

*STAR* splits a read and find the best portion that can be mapped for each piece. Then it maps the remaining portion, which can be far away in the case of a splice junction. The maximum mappable seed search looks for exact matches and uses the genome in the form of uncompressed suffix arrays. The second step of *STAR* stitches the seeds together within a given genomic window and allows mismatches, indels and splice junctions. The seeds from read pairs are handled concurrently at this step in order to increase sensitivity. [5, 13]

## 2.4 Count Algorithm

Read mapping results have to be summarized in terms of read coverage for genomic features of interest. Read counts are required for statistical methods like differential expression analysis. The approach of counting the number of mapped reads to annotation was accomplished by the program *featureCounts*.

*featureCounts* performs precise read assignment by comparing mapping location of every base in the read or fragment with the genomic region spanned by each feature. It takes account of any gaps like insertions, deletions, exon-exon junctions or

fusions) that are found in the read. The input for *featureCounts* consists of aligned reads in Sequence Alignment/Map (sam) or Binary Alignment/Map (bam) format and a list of genomic features in general feature format (gff). The read alignment and the feature annotation should correspond to the same reference genome, which is a set of reference sequences representing chromosomes or contigs. *featureCounts* supports strand-specific read counting with the option "-s".

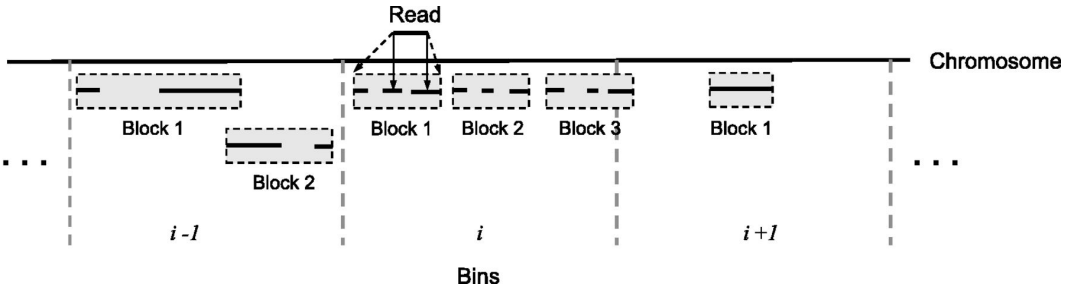


Figure 5: Approach of *featureCounts*: genome bins and feature blocks [16]

The algorithm is starting to generate a hash table for the reference sequence names. This enables that the reference sequence names are found to match in the input of sam/bam-files and gff-annotation quickly. Next the features in each reference sequence are sorted by their start position and a two-level hierarchy is created. Each chromosome is divided into non-overlapping 128kb bins. Features are assigned to bins according to their start positions and grouped into blocks within each bin. The query read is compared first with genomics bins, then with feature blocks within any overlapping bins and then with features in any overlapping blocks. This approach is shown in the illustration 5. [16]

## 2.5 Differential Expression Algorithm

Differential expression analysis refers to identification of genes or type of genomic features such as transcripts or exons, that are expressed in significantly different quantities in distinct groups of samples. In this study two sets of biological conditions, growth on toluene vs. growth on glucose, was compared by R/BioConductor packages *limma*.

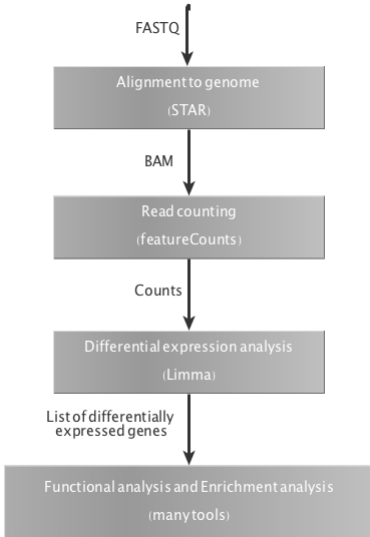


Figure 6: Steps of differential expression analysis

The first step of differential analysis is achieved by mapping RNA-seq data with *STAR* (2.3). The data input to *limma* should be counts such as reads-per-kilobase-per-million (RPKM) produced by *featureCounts* (2.4). *Limma* was then used to implement differential expression.

The software is based on the concept of linear models with the idea to model the expression of each gene as a linear combination of some different explanatory factors. For the experiment on *C. immunda* the linear model for each gene assembled by the measured gene expression ( $y$ ) is equal to the intercept ( $a$ ) representing the average expression level of the gene when the factor (*condition*) is in its reference state plus the error term ( $e$ ):

$$y = a + b * \text{condition} + e$$

A generalized linear model (GLM) is a more flexible version of a standard linear model that allows the distribution of the response variable to be different from the normal distribution used in standard linear regression. GLM assume that the read counts are distributed according to the negative binomial distribution. Accordingly the linear model should be written in matrix form, where the expression level ( $y$ ) is equal to experimental factor ( $X$ ) multiplied by the vector of parameters to be

estimated from the data ( $\beta$ ) plus the error term ( $\varepsilon$ ):

$$y = X * \beta + \varepsilon$$

Hence a contrast matrix has to be set up that describes which comparisons wants to be done. The advantages of *limma* is that it can account for more than one varying experimental factor using a generalized linear modelling framework, it is very fast and memory-intensive. [25]

## 2.6 Enrichment Approach

Through Enrichment Analysis a list of over-represented molecular functions, biological processes and cell locations, that can then be used to test whether genes are regulating biochemical or cellular pathway, is provided. Enrichment analysis is a necessary step after data analysis for more detailed annotations about differentially expressed genes, so that a biological meaning can be postulated.

Functional annotation elements are identified with R-packages Gene Set Enrichment Analysis (GSEA) [32] and Gene Ontology (GO) and the metabolic pathways by Kyoto Encyclopedia of Genes and Genomes (KEGG). A custom script was used to summarize the list of significantly overrepresented GO terms and data are graphically represented with R.

Gene Ontology classifies genes according to the biological process, cellular component and molecular function. It defines terms with gene products call GO terms, which are more or less detailed, depending on the state of knowledge or annotation. Each GO term has a term name, a unique identifier, the ontology it belongs to, synonyms including exact related ones and alternative unique identifiers, a definition including the source, a comment, the subset the terms belong to and community comments. The ontology is structured as a directed acyclic graph and each term has defined relationships to one or more other terms in the same domain. To keep in mind that the problem with using the GO terms is that a certain gene can map to several GO terms. [1]

Kyoto Encyclopedia of Genes and Genomes is a collection of databases dealing with biological pathways, genomes, diseases, drugs, and chemical substances. KEGG links genomic information with higher order functional information by computerizing current knowledge on cellular processes and by standardizing gene annotations. KEGG consists of three databases where the informations are stored. The genes database includes the genomic information, which is a collection of gene catalogs for all the completely sequenced genomes and some partial genomes with up-to-date annotation of gene functions. The higher order functional information is saved in the pathway database, which contains graphical representations of cellular processes, such as metabolism, membrane transport, signal transduction and cell cycle. The third one is the ligand database for the information about chemical compounds, enzyme molecules and enzymatic reactions. [12]

## 2.7 Pipeline implementation

The data used was downloaded from the sequencer-server, three of them were the transcriptomes of *Cladophialophora immunda* cultivated with glucose as carbon-source and the other three with toluene.

Before implementing the workflow system a comparison of publications, different programs and tools were done. The choice of a suitable program depended on the kind of analysis and the amount of time is required. Another important issue was the option available of the used program.

In the beginning the reads' origin was identified by aligning them to a reference genome with *STAR*. Mapped reads were used to perform transcript assembly with the softwares *Cufflinks* and *Trinity Genome Guided*. *Trinity* also was employed for mapping-free transcript assembly. With the produced assemblies from *Cufflinks* and *Trinity*, the Program to Assembly Spliced Alignments (*PASA*) performed the spliced alignment mapping. *PASA* assemblies were utilized to create hints for the location of introns and exons. Those hints were integrated in a hint-based run of *Augustus*. Evidence Modeler (*EVM*) was used to combine weighted predictions. The last step was a annotation update implemented by *PASA*, where the output of *EVM* compared to *PASA* alignment assemblies and generated a updated gene

set. [9, 29, 17]

Figure 7 shows the draft of the entire workflow system for genome annotation with transcriptomic data. The inputs are the transcriptomes from RNA-Seq in bam-format, the genome in fasta-format and the *deNovo* annotation data in gff3-format. After runs of the different steps the output is an annotation file in gff3-format.

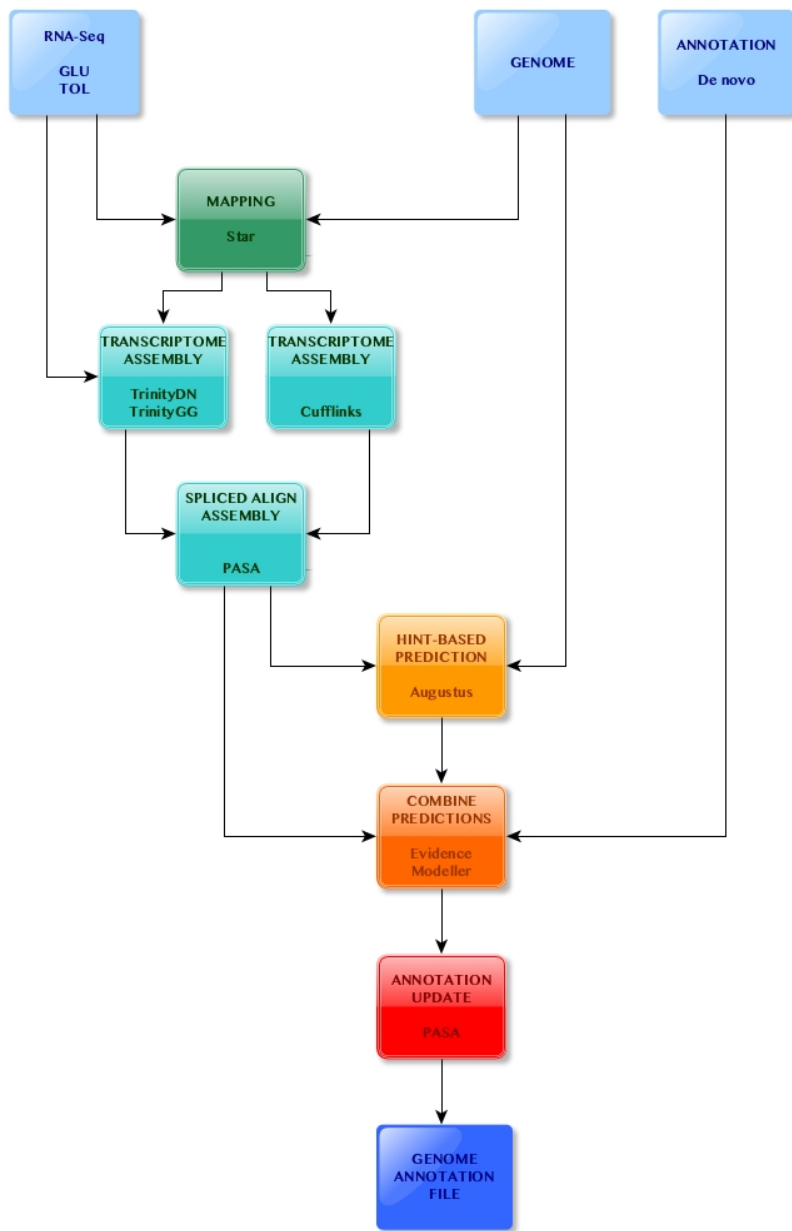


Figure 7: Genome annotation workflow system

## Mapping

### *STAR*

The execution of *STAR* allocated in two parts, building a reference index and mapping. Before running *STAR* mapping it was obtained a reference index of the genome. Mapping of the reads was executed without the soft clip aligning at reference ends. The mapped reads needed to be sorted by *Samtools*.

## Transcriptome Assembly

The goal of RNA-seq assembly is to reconstruct full-length transcripts based on sequenced reads. Transcript assembly answers the questions about exon regions and splice site. Several transcripts may overlap at different regions or there may be multiple copies of the same transcript.

There are two ways of performing transcriptome assembly. If there is a reference genome, it can be realised to guide the assembly, where the assembly task consists of solving which mapped reads correspond to which transcript. The second possibility is to perform *deNovo* assembly. [13]

### *Cufflinks*

The software packages *Cufflinks* can be used for *ab initio* reconstruction. The program within in this packages *Cufflinks* assembles transcriptomes from RNA-Seq data. *Cufflinks* reports the smallest possible set of isoforms. The program *Cuffmerge* was used to merge the multiple assembled transcriptomes into a master transcriptome. [33]

The rule *Cufflinks* was implemented with the following option and values: the maximum intron length (2000) and the minimum intron length (30), the maximum number of fragment a locus may have before skipped (10000) and the library-type ff-firststrand.

## ***Trinity***

*Trinity* consists of three separate programs: *Inchworm*, which construct initial contigs, *Chrysalis* which clusters the contigs produced by *Inchworm* and creates a de Bruijn Graph for each locus and *Butterfly*, which extracts the isoforms within each de Bruijn Graph. Each node of a de Bruijn Graph is associated with a (k -1)-mer. Two nodes A and B are connected if there is a k-mer whose prefix is the (k -1)-mer of the node A and the suffix is (k - 1)-mer of the node B. The k-mers create edges in the Buijn graph. [13] The k-mers is fixed to be 25 in *Trinity* the version 2.0.2. *Jellyfish* is the software, which calculates the k-mers and therefore maximum memory has to be defined. [20]

*Trinity* was executed genome-guided and *deNovo*. For genome-guided *Trinity* the mapped reads in bam-format and for the *deNovo* approach the raw reads in fastq-format were used. In both the option for strand-specific RNA-Seq read orientation for single end forward was required.

## ***PASA***

Program to Assembly Spliced Alignments (*PASA*) annotates protein-coding genes and alternatively splicing isoforms automatically. The goal of *PASA* is to find for each alignment the largest assembly, which is used to create gene models or to modify existing gene models. [7] Further reconstructed assemblies are the input into *PASA* tool. Then *PASA* aligns these newly assembled transcripts to the genome using the software *GMAP*. Next *PASA* filters invalid alignments and those transcripts more likely resulting as artifacts of the RNA-seq assembly process and reconstructs more complete transcripts using its alignment assembly algorithm. [9]

The reconstructed inputs for the *PASA* run were *Trinity deNovo* assemblies, *Trinity genome-guided* assemblies and *Cufflinks* transcript structures.

## Gene Prediction

### *Augustus*

*Augustus* is an *ab initio* gene predictor, where only a genomic sequence is needed as input information. In addition it is possible to use hints of various information. For the prediction *Augustus* combines genomic sequence alignments and alignments of expressed sequenced tags (EST).

Expressed Sequence Tag (EST) was evolved in early days of genome assembly. First the same assemblers were used for transcriptomes, but there are fundamental differences between genome assembly and transcriptome assembly. In the genome assembly the ideal output is a linear sequence representing each genomic region, whereas in the transcriptome assembly the gene is most naturally described as a graph. [13]

The model underlying the program is generalized hidden Markov model (GHMM). HMMs and GHMMs for gene prediction define a probability for each pair  $(\varphi, s)$  of a sequence ( $s$ ) and a gene structure ( $\varphi$ ). Before starting the program *Augustus* it is necessary to train the model. [28]

The training set was created from *PASA* assemblies by executing the program "pasa\_asmbls\_to\_training\_set.dbi" included in *PASA* package. For the additional file of hints the location of introns were filtered from *PASA* assemblies. Subsequently *Augustus* was started and after more than 24 hours, the output was a complete gene prediction in ggf-format.

### *Evidence Modeler*

The Evidence Modeler (*EVM*) is an automated eukaryotic gene structure annotation tool. *EVM* reports eukaryotic gene structures by using weighted evidence combining technique. The evidence utilized by *EVM* corresponds to *ab initio* gene predictions and transcript alignment. [8]

The assembly of *PASA* (weight = 10), the *Augustus* prediction (weight = 5) and the *deNovo* Annotation (weight = 1) were combined by *EVM*.

### ***Pasa Annotation Update***

Again Program to Assembly Spliced Alignments (*PASA*) was used to update the *EVM* consensus prediction by adding UTR annotations and models for alternatively spliced isoforms.

# Results

The average mean read length was 140,5M and the total reads generated per sample varied between 85,080,007 and 94,144,127.

Samples	Total Reads	Mean Read Length
GLU1	85.1M	133
GLU2	94.1M	147
GLU3	85.8M	140
TOL1	87.8M	159
TOL2	78.0M	134
TOL3	84.6M	130

Table 2: RNA Sequencing Read Summary

## 3.1 Up- and Down-regulated genes

All the steps for analysing the expressed genes are called downstream analysis. In the last step of statistical determination the data was separated in up- and down-regulated genes. For the up-regulated data set threshold was set by a p-value less than 0.2 and the logFC-value (logFoldChange) greater than zero. For the down-regulated dataset threshold was set again by a p-value less than 0.2 but an logFC-value less than or equal to zero.

The logFC-value is used to determine two data sets reflecting gene expression measured under different conditions, e.g. if the result is 0.2, it means that the expression level in the experimental condition (TOL-samples) is 0.2-fold the expression as in the control condition (GLU-samples).

## 10 most Up- and Down-regulated genes

geneID	logFC	AveExpr	t	P.Value	adj.P.Val	B
JSEJ01000027.1.121	9,157671427	11,01902243	34,19677788	4,59E-17	3,92E-13	28,15287351
JSEJ01000048.1.3	8,135554813	11,15870924	30,84561682	2,56E-16	1,09E-12	26,80565492
JSEJ01000128.1.27	8,264361041	8,24645472	26,0280989	4,29E-15	1,22E-11	24,15678934
JSEJ01000047.1.83	6,143951797	9,487939172	24,95531824	8,60E-15	1,54E-11	23,82051174
JSEJ01000040.1.6	8,353205867	6,693442984	24,88192941	9,03E-15	1,54E-11	23,18910965
JSEJ01000118.1.44	6,055216556	10,15304114	23,86371332	1,80E-14	2,56E-11	23,16026207
JSEJ01000012.1.35	5,977114267	12,65195266	23,00250399	3,29E-14	3,29E-11	22,58014797
JSEJ01000031.1.43	6,754060011	11,71227935	22,92972613	3,47E-14	3,29E-11	22,54452776
JSEJ01000113.1.50	8,03548922	10,60107357	22,57155602	4,49E-14	3,83E-11	22,30063571
JSEJ01000070.1.66	8,508993803	6,164674619	22,2024474	5,89E-14	4,24E-11	21,53678647

Table 3: 10 most Up-regulated genes

geneID	logFC	AveExpr	t	P.Value	adj.P.Val	B
JSEJ01000100.1.24	-7,498665272	7,747744106	-22,98902806	3,32E-14	3,29E-11	22,30611909
JSEJ01000161.1.20	-8,866531212	6,185450242	-21,75485658	8,22E-14	4,24E-11	21,14599408
JSEJ01000037.1.86	-5,635055473	8,551635429	-21,08356096	1,37E-13	5,58E-11	21,25535901
JSEJ01000146.1.21	-5,064637844	9,170287113	-19,05864813	7,10E-13	1,73E-10	19,74278703
JSEJ01000071.1.25	-6,174423645	7,057845126	-18,85738485	8,44E-13	1,95E-10	19,43283451
JSEJ01000079.1.8	-5,546577865	9,934645785	-18,34271713	1,32E-12	2,50E-10	19,14942065
JSEJ01000003.1.28	-5,718439007	7,347779099	-17,74081308	2,26E-12	3,47E-10	18,55773184
JSEJ01000022.1.51	-7,925562894	6,932767343	-17,42614263	3,02E-12	4,16E-10	18,15011866
JSEJ01000125.1.1	-5,054168871	6,687468173	-17,19210644	3,75E-12	4,78E-10	18,06479201
JSEJ01000039.1.91	-4,286585186	10,59182994	-16,99691044	4,50E-12	5,47E-10	17,97012785

Table 4: 10 most Down-regulated genes

Overall, there are 501 genes differentially expressed.

To visualize the correlation of the samples and check for potential outliers a correlation heatmap and principal component (PCA) plot was created.

Heatmap using a color scale to displays the expression values of the genes. Genes are arranged in columns (samples) and rows (features) as in the data matrix. Each feature-sample pair is represented with a small rectangle that is coloured according to its expression.

The results of the correlation between the different samples are presented in the heatmap in figure 8a. The dendrograms along the sides show how the samples and the features are independently clustered. Light colour like yellow indicates a good

relation between the samples. The darker the colour, the lower is the correlation. Principal component analysis is based on finding which samples have the strongest correlation. As figure 8b shows a variance of 94% between the glucose and toluene samples. On y-axis the variance between the samples is 2%.

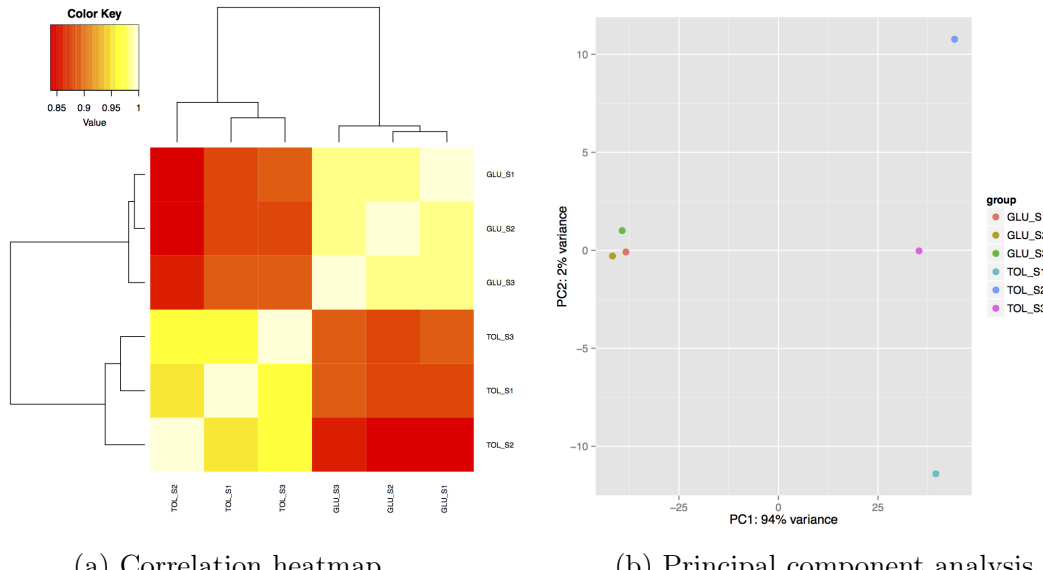


Figure 8: Correlation analysis

## 3.2 Functional enrichment

### 3.2.1 Gene Ontology

Gene Ontology analysis represent the major and minor changes in biological process, cellular component and molecular function.

ID	P-value	OddsRatio	ExpCount	Count	Size	Term	FDR
GO:0019538	8,97E-06	2,363104312	19,74720125	40	786	protein metabolic process	0,001948953
GO:0044267	9,21E-06	2,498080515	16,20476438	35	645	cellular protein metabolic process	0,001948953
GO:0006457	4,62E-05	7,153393393	1,331554283	8	53	protein folding	0,00650895
GO:0043170	0,000235609	1,714121695	57,0055975	80	2269	macromolecule metabolic process	0,024915629
GO:0044260	0,000353588	1,698863684	53,11142932	75	2114	cellular macromolecule metabolic process	0,029913529
GO:0009987	0,000500955	1,678863549	111,5490758	134	4440	cellular process	0,035317296
GO:0006259	0,000641171	3,128205128	4,57250716	13	182	DNA metabolic process	0,038745034
GO:0050896	0,001207766	2,309548097	9,471621973	20	377	response to stimulus	0,059594894
GO:0036211	0,001408863	2,39001387	8,215438688	18	327	protein modification process	0,059594894
GO:0006464	0,001408863	2,39001387	8,215438688	18	327	cellular protein modification process	0,059594894
GO:0051716	0,001556564	2,432672441	7,612470711	17	303	cellular response to stimulus	0,059856958
GO:0043412	0,001812698	2,274957274	9,094766988	19	362	macromolecule modification	0,060287023
GO:0006515	0,001852793	78,40837696	0,075370997	2	3	misfolded or incompletely synthesized protein catabolic process	0,060287023
GO:0006950	0,002149255	2,837258893	4,597630825	12	183	response to stress	0,0649382
GO:0006281	0,002347231	3,406839623	2,889221557	9	115	DNA repair	0,065846628
GO:0006974	0,002490653	3,374542869	2,914345223	9	116	cellular response to DNA damage stimulus	0,065846628
GO:0043038	0,003061277	5,664133739	1,004946628	5	40	amino acid activation	0,068153683
GO:0043039	0,003061277	5,664133739	1,004946628	5	40	tRNA aminoacylation	0,068153683
GO:0006418	0,003061277	5,664133739	1,004946628	5	40	tRNA aminoacylation for protein translation	0,068153683
GO:0033554	0,00331557	3,221710016	3,039963551	9	121	cellular response to stress	0,068335305
GO:0044237	0,003392533	1,503857005	73,28573288	92	2917	cellular metabolic process	0,068335305
GO:0071704	0,00385927	1,490845061	82,33025254	101	3277	organic substance metabolic process	0,074203235
GO:0016569	0,004632185	10,73397129	0,35173132	3	14	covalent chromatin modification	0,081642257

Table 5: Overrepresented GO terms for the genes up-regulated

The results, as shown in table 5, indicate that there are changes in the protein metabolic process and cellular protein metabolic process. There is an impact on the chemical reactions and pathways involving a specific protein, rather than of proteins in general.

Protein folding is the next up-regulated process, which affect the chaperone activity. Chaperones assist in the covalent and non-covalent assembly of single chain polypeptides into the correct tertiary structure.

Furthermore the metabolic processes of macromolecules, cellular macromolecules,

DNA and the protein modification process are up-regulated. The significance of these processes is lower than in the first three processes. In figure 9 the results obtained from the GO terms for up-regulated genes are presented.

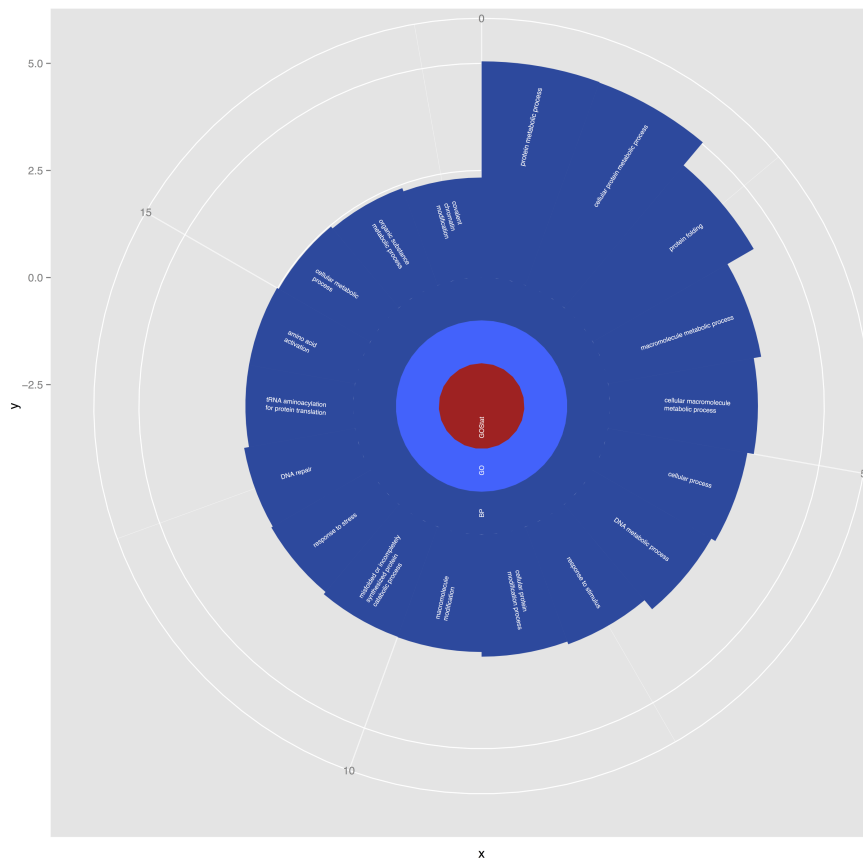


Figure 9: GO terms for up-regulated genes

ID	P-value	OddsRatio	ExpCount	Count	Size	Term	FDR
GO:0006412	1,40E-25	9,962993421	6,69317886	45	197	translation	8,67E-23
GO:0006091	6,42E-20	28,14456522	1,494923197	21	44	generation of precursor metabolites and energy	1,99E-17
GO:0046128	4,66E-15	21,47353142	1,392996615	17	41	purine ribonucleoside metabolic process	7,24E-13
GO:0042278	4,66E-15	21,47353142	1,392996615	17	41	purine nucleoside metabolic process	7,24E-13
GO:0009199	1,15E-14	28,22027439	1,053241343	15	31	ribonucleoside triphosphate metabolic process	1,01E-12
GO:0009144	1,15E-14	28,22027439	1,053241343	15	31	purine nucleoside triphosphate metabolic process	1,01E-12
GO:0009205	1,15E-14	28,22027439	1,053241343	15	31	purine ribonucleoside triphosphate metabolic process	1,01E-12
GO:0046034	1,30E-14	34,99527665	0,883363707	14	26	ATP metabolic process	1,01E-12
GO:0044281	2,50E-14	3,67855516	20,96290029	60	617	small molecule metabolic process	1,73E-12
GO:0009141	3,74E-14	25,07791328	1,121192398	15	33	nucleoside triphosphate metabolic process	2,32E-12
GO:0072521	2,67E-13	12,3180939	2,242384796	19	66	purine-containing compound metabolic process	1,43E-11
GO:0009167	2,99E-13	20,50720621	1,257094507	15	37	purine ribonucleoside monophosphate metabolic process	1,43E-11
GO:0009126	2,99E-13	20,50720621	1,257094507	15	37	purine nucleoside monophosphate metabolic process	1,43E-11
GO:0009119	3,35E-13	15,13729508	1,732751888	17	51	ribonucleoside metabolic process	1,49E-11
GO:0015980	4,19E-13	29,87096774	0,883363707	13	26	energy derivation by oxidation of organic compounds	1,74E-11
GO:0045333	8,81E-13	35,71566265	0,747461599	12	22	cellular respiration	3,42E-11
GO:0009150	1,70E-12	15,07959184	1,630825306	16	48	purine ribonucleotide metabolic process	6,21E-11
GO:0019693	2,45E-12	14,62065553	1,664800833	16	49	ribose phosphate metabolic process	8,00E-11
GO:0009259	2,45E-12	14,62065553	1,664800833	16	49	ribonucleotide metabolic process	8,00E-11
GO:0009161	2,70E-12	16,69828365	1,426972143	15	42	ribonucleoside monophosphate metabolic process	8,39E-11
GO:0009123	5,92E-12	15,54247267	1,494923197	15	44	nucleoside monophosphate metabolic process	1,75E-10
GO:0044711	9,25E-12	4,11027424	11,9933611	40	353	single-organism biosynthetic process	2,59E-10
GO:0006163	9,60E-12	13,032984	1,800702942	16	53	purine nucleotide metabolic process	2,59E-10
GO:0009116	1,86E-11	9,169749442	2,785993231	19	82	nucleoside metabolic process	4,82E-10
GO:1901657	2,35E-11	9,025245351	2,819968758	19	83	glycosyl compound metabolic process	5,83E-10
GO:0006818	2,93E-11	18,47158218	1,155167925	13	34	hydrogen transport	6,75E-10
GO:0015992	2,93E-11	18,47158218	1,155167925	13	34	proton transport	6,75E-10
GO:0042451	5,71E-11	20,98936924	0,985290289	12	29	purine nucleoside biosynthetic process	1,22E-09
GO:0046129	5,71E-11	20,98936924	0,985290289	12	29	purine ribonucleoside biosynthetic process	1,22E-09
GO:1902600	9,24E-11	19,8206158	1,019265816	12	30	hydrogen ion transmembrane transport	1,91E-09
GO:0098660	2,05E-10	9,163129391	2,480213486	17	73	inorganic ion transmembrane transport	3,85E-09
GO:0098662	2,05E-10	9,163129391	2,480213486	17	73	inorganic cation transmembrane transport	3,85E-09
GO:0098655	2,05E-10	9,163129391	2,480213486	17	73	cation transmembrane transport	3,85E-09
GO:0044267	2,39E-10	3,014787023	21,91421505	54	645	cellular protein metabolic process	4,36E-09
GO:0009117	3,44E-10	6,995755234	3,635381411	20	107	nucleotide metabolic process	6,11E-09
GO:0015672	3,82E-10	10,71283391	1,936605051	15	57	monovalent inorganic cation transport	6,59E-09
GO:0009142	4,38E-10	26,83810214	0,713486071	10	21	nucleoside triphosphate biosynthetic process	6,64E-09
GO:0009145	4,38E-10	26,83810214	0,713486071	10	21	purine nucleoside triphosphate biosynthetic process	6,64E-09
GO:0009201	4,38E-10	26,83810214	0,713486071	10	21	ribonucleoside triphosphate biosynthetic process	6,64E-09

Table 6: Overrepresented GO terms for the genes down-regulated

The biological process of translation is down-regulated. Translation is the synthesis of proteins and therefore one of the most important process within a cell. The chemical reactions and pathways resulting in the formation of precursor metabolites and substances, from which energy is derived, are also down-regulated. As can be seen in table 6, most overrepresented GO terms belong to the purine nucleoside metabolic process. A nucleoside or ribonucleoside bound to a triphosphate are also known as GTP (guanosine triphosphate) or ATP (adenosine triphosphate) and are necessary for cell metabolism and regulation, especially those involving DNA and RNA synthesis. They act as energy source or activator for substrates. Additionally, genes for the ATP metabolic process and the proton transport are lower expressed significantly. The mentioned processes belong to generation of energy.

In figure 9 the results obtained from the GO terms for lower expressed genes are presented. Similar processes, like purine ribonucleoside metabolic process and purine nucleoside metabolic process, are grouped together.

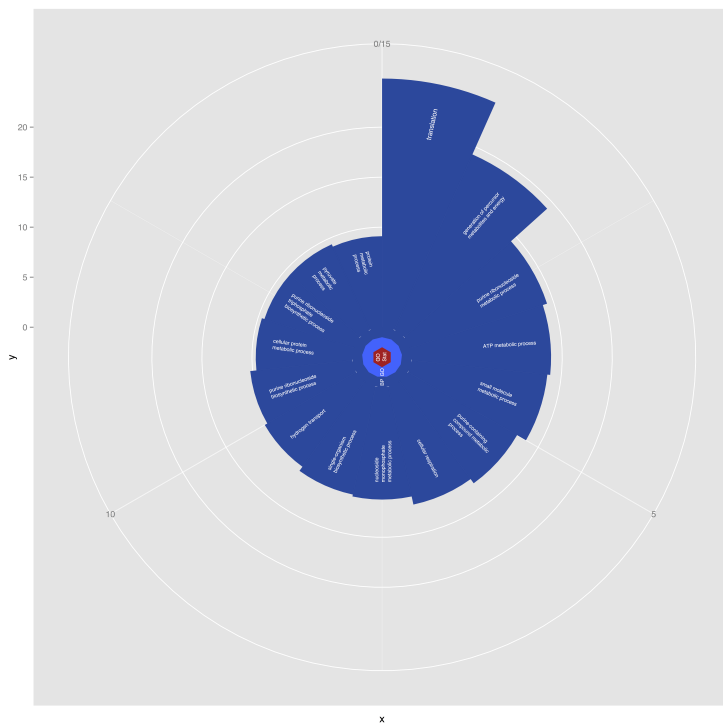


Figure 10: GO terms for down-regulated genes

### 3.2.2 KEGG

ID	P-value	OddsRatio	ExpCount	Count	Size	FDR	Fenes
ko00020	0,000297044	30,4	0,436363636	4	6	0,008614271	JSEJ01000010.1.81 JSEJ01000023.1.136 JSEJ01000099.1.18 JSEJ01000099.1.19
ko00660	0,00065906	20,2	0,509090909	4	7	0,009556376	JSEJ01000010.1.81 JSEJ01000023.1.136 JSEJ01000099.1.18 JSEJ01000099.1.19
ko00010	0,001298374	43,57142857	0,290909091	3	4	0,012550945	JSEJ01000039.1.14 JSEJ01000027.1.103 JSEJ01000074.1.37

Table 7: Overrepresented KEGG pathways for the genes down-regulated

In contrast to GO analysis, KEGG terms was only found for genes down-regulated. Genes related to pathways of TCA cycle, carbohydrate metabolism and Glycolysis/Gluconeogenis were lower expressed. These pathways are assigned to carbohydrate and energy categories that function in catabolism.

Four genes are differentially expressed in TCA cycle and in C5-branched dibasic acid metabolism. TCA cycle is a central metabolic pathway that completes the oxidative degradation of carbohydrates, amino acids and fatty acids. The energy generated in this cycle is in the form of GTP and ATP.

Glycolysis/Gluconeogenesis provide the catabolized nutrients as substrates for TCA cycle and C5-branched dibasic acid metabolism. In glycolysis glucose is broken down in pyruvate by production of ATP. Gluconeogenesis is the biosynthesis of glucose from pyruvate and therefore the reverse anabolic process and equal important as glycolysis.

Taken together, these results of down-regulated pathways suggests a general shutdown of carbohydrate catabolism and energy generation.

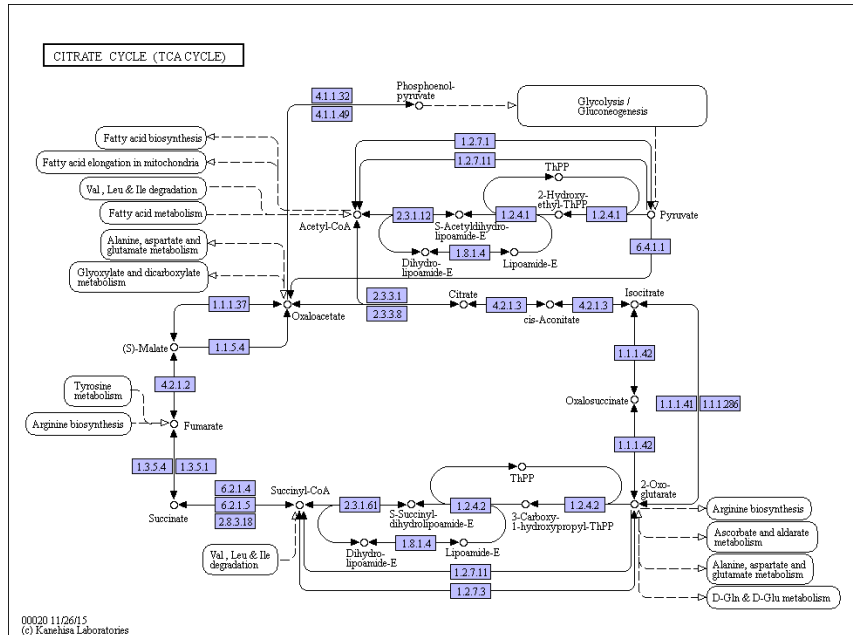


Figure 11: KEGG pathway of TCA cycle

### 3.2.3 Differentially expressed proteins

Results of differentially expressed proteins were generated with different databases and sequence analysing tools (Pfam, Interpro, UniPath, superfam,...).

Genes coding for the specific protein Hsp 20 which belong to the family of heat shock proteins are significantly higher expressed. The synthesis of this proteins is the responds to environmental stress. Heat shock proteins act as protein chaperones that can protect protein against denaturation and aggregation. [27] [19] The synthesis of terminal and central domain of chaperone DnaJ (Hsp 40) is higher expressed too.

Further analysis confirm the up-regulation of proteins coding for HSP20-like chaperones, HSP40/DnaJ peptide-binding and Hsp20 domain. Zinc finger domains (RING/FYVE/PHD-type, CCCH-type) are represented strongly. Zinc finger domains are known as a DNA-binding motif and are involved in transcriptional processes.

It is necessary to mention that protein coding for AAA+ ATPase domain and AT-

Pase AAA-type core also are up-regulated. AAA+ ATPase domain participate in diverse cellular processes including membrane fusion, proteolysis and DNA replication. ATPase AAA-type core function as molecular chaperones and act as DNA helicases and transcription factor.

In line with the results of KEGG pathway analysis, the enzymes citrate synthase, ATP synthase and CoA-ligase are down-regulated.

Citrate synthase catalysis the first reaction in the TCA cycle, the conversion of oxalacetate and acetyl-coenzyme A into citrate and coenzyme A. This reaction is important for energy generation and for carbon assimilation. ATP synthases are a membrane-bound enzyme complexes and ion transporters that combine ATP synthesis and hydrolysis with the transport of protons across the membrane. CoA-ligase is part of succinyl-CoA synthetase and this enzyme belong to TCA cycle. Another lower expressed enzyme is chitin synthase. Chitin synthase catalyzes the conversion of UDP-N-acetyl-D-glucosamine to UDP. UDP is an important factor in gluconeogenesis.

### 3.3 Toluene Degradation

The result of the previous studies indicate that the increase of CO<sub>2</sub> concentration come along with the degradation of toluene. Therefore the focus of the results is on the enzymes of the toluene-degradation-pathway. Table 8 shows the summary statistic for the enzymes of toluene degradation.

Enzymes		logFC	P.Value	adj.P.Value
<b>P450</b>	Cytochrome-P-450 toluene	1.2991421176278	4.76275764901422x10 <sup>-5</sup>	0.00015206178906281
<b>BADH</b>	Benzyl-Alcohol-Dehydrogenase	-0.610068198027962	0.0215490685115476	0.0341873128136395
<b>BZDH</b>	Benzal-Dehydrogenase	1.29914211762787	4.76275764901422x10 <sup>-5</sup>	0.000152061789062813
<b>BH</b>	hypothetical-Benzoate-Hydroxylase			
<b>PHBH</b>	p-hydroxybenzoate-Hydroxylase	5.52538725225511	1.45988708444616x10 <sup>-10</sup>	7.61270285910155x10 <sup>-9</sup>
<b>PCAD</b>	Protocatechuate-Dioxygenase			
<b>C12O</b>	Catechol-1-2-Dioxygenase	2.86929824283322	2.88989072866634x10 <sup>-6</sup>	1.43614755006986x10 <sup>-5</sup>
<b>MLE</b>	cis-cis-Muconate-Lactonizing-Enzyme	1.28113181586883	0.00654904836295034	0.0117901712197061
<b>MI</b>	Mucolactone-Isomerase	1.6912116141732	0.00111759914912401	0.0024233473897696
<b>EHL</b>	$\beta$ -ketoAdipateEnol-LactoneHydrogenase	-0.883899764697411	0.0121983401347394	0.0205651854673907
<b>P340</b>	Protocatechuate-Dioxygenase			
<b>CMLE</b>	$\beta$ -Carboxy-cis-cis-Muconate-Lactonizing-Enzyme	1.28113181586883	0.00654904836295034	0.0117901712197061
<b>CMH</b>	$\beta$ -Carboxymuconate-Enzyme	1.28113181586883	0.00654904836295034	0.011790171219706
<b>TR</b>	$\beta$ -ketoadipat-CoA-Transferase	-0.868139308745568	0.0167231462329001	0.0272631578512478
<b>TH</b>	$\beta$ -ketoadipyl-CoA-Thiolase	2.2148894022903	2.73997262728265x10 <sup>-7</sup>	2.13649579005871x10 <sup>-6</sup>

Table 8: Enzymes of toluene degradation

The initial oxidation on the methyl group of toluene is catalyzed by cytochrome P-450 monooxygenase (P450) to form benzyl alcohol, which is then converted to benzaldehyde and benzoate by the relevant dehydrogenases (BADH and BZDH). Benzoate is then apparently hydroxylated (BH) to form p-hydroxybenzoate, which is oxidized by p-hydroxybenzoate hydroxylase (PHBH) to protocatechuate. At this stage there are two options, both of which may be occurring simultaneously. Since the organism has P340 activity (P340), protocatechuate is likely being metabolized through an ortho-cleavage pathway, which has been seen previously in other fungi. However, since C12O (C120) activity is also present in toluene-grown cells, protocatechuate may be decarboxylated to catechol, which is then oxidized through the other branch of the  $\beta$ -ketoadipate pathway. The conversion of  $\beta$ -carboxymuconate to  $\beta$ -ketoadipate involves the participation of two enzymes (CMLE and CMH). [21]

All except three enzymes (BADH, EHL and TR) of toluene-degradation pathway are up-regulated. The enzyme with the highest activity is p-hydroxybenzoate hydroxylase. Enzyme C120 is higher expressed too.

The end products of toluene degradation (Succinyl-CoA and Acetyl-CoA) are utilized as substrates for the TCA cycle.

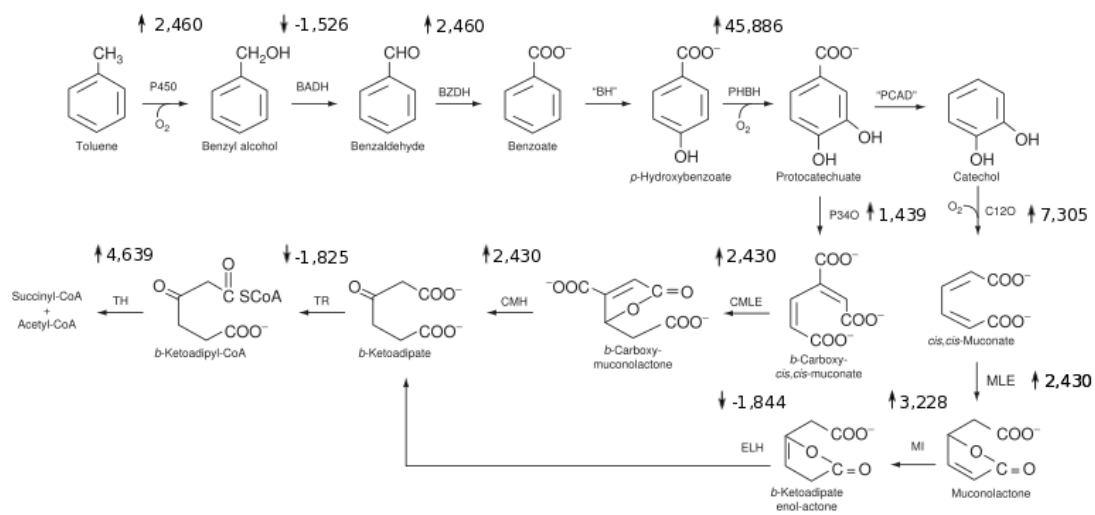


Figure 12: Toluene degradation pathway

# Discussion

The study was designed to determine the effect of toluene of *C. immunda* at transcriptome level. The results has shown that translation is significantly down-regulated. Many biological processes regarding to the purine nucleoside metabolic process are also lower expressed compared to glucose-samples. This has an effect on the cell metabolism and energy generation.

Interestingly, the genes coding for specific protein metabolic processes and protein folding are highly expressed. These results suggest that the cell can survive by building proteins for protection like chaperones or heat shock proteins. But the cell slow down the processes of RNA synthesis and subsequent protein synthesis. Overall, the results of GO enrichment and KEGG pathways analysis revealed a coordinated shutdown of metabolic activity at the transcript level.

This study has found that generally the genes for toluene degradation are up-regulated. This results support the idea that *C. immunda* use toluene as carbon and energy source. It can therefore be assumed that the missing catabolites from glycolysis and glycogenolyses are provided by the products of toluene degradation. Hence this could be important for the cell to survive in such extreme environments.

Another interesting result for further studies is the up-regulation of genes coding for DNA-binding motifs like Zinc finger. This finding has important implications for determinations on human pathogenicity and therapeutic genes in black yeasts, e.g. Zinc finger domains bind selectively to specific sequences of DNA.

# Conclusion

The aim of this work was to analyse the transcriptome of *Cladophialophora immunda*. This extremophilic organism is an important fungi with the ability to degrade toluene. *Cladophialophora immunda* can use toluene as carbon and energy source and provide these catabolites as substrates for TCA cycle.

For analysis a genome annotation pipeline with RNA-seq data as input was developed. This pipeline allows a fast production of differentially expressed data. It should be noted that the used softwares and differential expression analysis methods for RNA-seq are still under active development.

Possibilities of the ongoing research could be a closer look at enzymes of toluene degradation pathway or special proteins by PCR methods to getting a deeper understanding of the black yeasts as special *Cladophialophora immunda*.

The equipment of the VIBT-Extremophile Center used in this study was financed by BOKU-Equipment GesmbH. The computational results presented have been achieved in part using the Vienna Scientific Cluster (VSC).

# Bibliography

- [1] Michael Ashburner, Catherine A Ball, Judith A Blake, David Botstein, Heather Butler, J Michael Cherry, Allan P Davis, Kara Dolinski, Selina S Dwight, Janan T Eppig, Midori A Harris, David P Hill, Laurie Issel-Tarver, Andrew Kasarskis, Suzanna Lewis, John C Matese, Joel E Richardson, Martin Ringwald, Gerald M Rubin, and Gavin Sherlock. Gene Ontology: tool for the unification of biology. *Nat Genet*, 25(1):25–29, may 2000.
- [2] H. Badali, C. Gueidan, M. J. Najafzadeh, a. Bonifaz, a. H G Gerrits van den Ende, and G. S. de Hoog. Biodiversity of the genus Cladophialophora. *Studies in Mycology*, 61:175–191, 2008.
- [3] Barbara Blasi, Caroline Poyntner, Tamara Rudavsky, Francesc X. Prenafeta-Boldú, Sybren de Hoog, Hakim Tafer, and Katja Sterflinger. Pathogenic yet environmentally friendly? Black fungal candidates for bioremediation of pollutants. *Geomicrobiology Journal; inPress*, 2015.
- [4] Barbara Blasi, Hakim Tafer, Donatella Tesei, and Katja Sterflinger. From Glacier to Sauna: RNA-Seq of the Human Pathogen Black Fungus Exophiala dermatitidis under Varying Temperature Conditions Exhibits Common and Novel Fungal Response. *Plos One*, 10(6):e0127103, 2015.
- [5] Alexander Dobin, Carrie a. Davis, Felix Schlesinger, Jorg Drenkow, Chris Zaleski, Sonali Jha, Philippe Batut, Mark Chaisson, and Thomas R. Gineras. STAR: Ultrafast universal RNA-seq aligner. *Bioinformatics*, 29(1):15–21, 2013.
- [6] Cene Gostinčar, Martin Grube, Sybren De Hoog, Polona Zalar, and Nina

Gunde-Cimerman. Extremotolerance in fungi: Evolution on the edge. *FEMS Microbiology Ecology*, 71(1):2–11, 2010.

- [7] B. J. Haas. Improving the *Arabidopsis* genome annotation using maximal transcript alignment assemblies. *Nucleic Acids Research*, 31(19):5654–5666, oct 2003.
- [8] Brian J Haas, Steven L Salzberg, Wei Zhu, Mihaela Pertea, Jonathan E Allen, Joshua Orvis, Owen White, C Robin Buell, and Jennifer R Wortman. Automated eukaryotic gene structure annotation using EVidenceModeler and the Program to Assemble Spliced Alignments. *Genome biology*, 9(1):R7, 2008.
- [9] Brian J Haas, Qiandong Zeng, Matthew D Pearson, Christina a Cuomo, and Jennifer R Wortman. Approaches to Fungal Genome Annotation. *Mycology*, 2(3):118–141, 2011.
- [10] S. Hartmans and J. Tramper. Dichloromethane removal from waste gases with a trickle-bed bioreactor. *Bioprocess Engineering*, 6(3):83–92, feb 1991.
- [11] G S De Hoog, V Vicente, R B Caligorne, S Kantarcioglu, K Tintelnot, and G Haase. Species Diversity and Polymorphism in the. 41(10):4767–4778, 2003.
- [12] Minoru Kanehisa and Susumu Goto. KEGG: Kyoto Encyclopaedia of Genes and Genomes. *Nucl. Acids Res.*, 28(1):27–30, 2000.
- [13] Eija Korpelainen, Jarno Tuimala, Panu Somervuo, Mikael Huss, and Garry Wong. *RNA-seq Data Analysis: A Practical Approach*. 2015.
- [14] Johannes Köster and Sven Rahmann. Snakemake-a scalable bioinformatics workflow engine. *Bioinformatics*, 28(19):2520–2522, 2012.
- [15] Heng Li and Nils Homer. A survey of sequence alignment algorithms for next-generation sequencing. *Briefings in bioinformatics*, 11(5):473–83, sep 2010.
- [16] Yang Liao, Gordon K. Smyth, and Wei Shi. FeatureCounts: An efficient general purpose program for assigning sequence reads to genomic features, 2014.

- [17] J. Linde, S. Duggan, M. Weber, F. Horn, P. Sieber, D. Hellwig, K. Riege, M. Marz, R. Martin, R. Guthke, and O. Kurzai. Defining the transcriptomic landscape of *Candida glabrata* by RNA-Seq. *Nucleic Acids Research*, 43(3):1392–1406, 2015.
- [18] Dion M.a.M Luykx, Francesc X Prenafeta-Boldú, and Jan a.M de Bont. Toluene monooxygenase from the fungus *Cladosporium sphaerospermum*. *Biochemical and Biophysical Research Communications*, 312(2):373–379, 2003.
- [19] Halim Maaroufi and Robert M Tanguay. Analysis and Phylogeny of Small Heat Shock Proteins from Marine Viruses and Their Cyanobacteria Host. *PLoS ONE*, 8(11):e81207, nov 2013.
- [20] Nir Manfred G. Grabherr, Brian J. Haas, Moran Yassour, Joshua Z. Levin, Dawn A. Thompson, Ido Amit, Xian Adiconis, Lin Fan, Raktima Raychowdhury, Qiandong Zeng, Zehua Chen, Evan Mauceli, Nir Hacohen, Andreas Gnirke, Nicholas Rhind, Federica di Palma, Bruce W., Friedman, and Aviv Regev. Trinity: reconstructing a full-length transcriptome without a genome from RNA-Seq data. *Nature Biotechnology*, 29(7):644–652, 2013.
- [21] R. E. Parales, J. V. Parales, D. A. Pelletier, and J. L. Ditty. Chapter 1 Diversity of Microbial Toluene Degradation Pathways. *Advances in Applied Microbiology*, 64:1–73, jan 2008.
- [22] Caroline Poyntner. *Bioremediation of waste gas and soil by black extremotolerant fungi*. PhD thesis, 2014.
- [23] Francesc X. Prenafeta-Boldú, Andrea Kuhn, Dion M.A.M. Luykx, Heidrun Anke, Johan W. van Groenestijn, and Jan A.M. de Bont. Isolation and characterisation of fungi growing on volatile aromatic hydrocarbons as their sole carbon and energy source. *Mycological Research*, 105(4):477–484, apr 2001.
- [24] Noura Raddadi, Ameur Cherif, Daniele Daffonchio, Mohamed Neifar, and Fabio Fava. Biotechnological applications of extremophiles, extremozymes and extremolytes. *Applied Microbiology and Biotechnology*, pages 7907–7913, 2015.

- [25] M. E. Ritchie, B. Phipson, D. Wu, Y. Hu, C. W. Law, W. Shi, and G. K. Smyth. limma powers differential expression analyses for RNA-sequencing and microarray studies. *Nucleic Acids Research*, 43(7):e47–e47, 2015.
- [26] L J Rothschild and R L Mancinelli. Life in extreme environments. *Nature*, 409(September 2000):1092–1101, 2001.
- [27] S Lindquist and and E A Craig. The Heat-Shock Proteins. *Annual Review of Genetics*, 22(1):631–677, 1988.
- [28] Mario Stanke, Ana Tzvetkova, and Burkhard Morgenstern. AUGUSTUS at EGASP: using EST, protein and genomic alignments for improved gene prediction in the human genome. *Genome biology*, 7 Suppl 1(May 2005):S11.1–8, 2006.
- [29] Tamara Steijger, Josep F. Abril, Pär G. Engström, Felix Kokocinski, The RGASP Consortium, Tim J. Hubbard, Roderic Guigó, Jennifer Harrow, and Paul Bertone. Assessment of transcript reconstruction methods for RNA-seq. *Nature Methods*, 10(12):1177–1184, 2013.
- [30] Katja Sterflinger. Black Yeasts and Meristematic Fungi: Ecology, Diversity and Identification. In Gábor Péter and Carlos Rosa, editors, *Biodiversity and Ecophysiology of Yeasts SE - 20*, The Yeast Handbook, pages 501–514. Springer Berlin Heidelberg, 2006.
- [31] Katja Sterflinger, Ksenija Lopandic, Barbara Blasi, Caroline Poynter, and Sybren De Hoog. Draft Genome of Cladophialophora immunda , a Black Yeast and Efficient Degrader of Polyaromatic Hydrocarbons. 3(1):5–6, 2015.
- [32] Aravind Subramanian, Pablo Tamayo, Vamsi K Mootha, Sayan Mukherjee, Benjamin L Ebert, Michael a Gillette, Amanda Paulovich, Scott L Pomeroy, Todd R Golub, Eric S Lander, and Jill P Mesirov. Gene set enrichment analysis: a knowledge-based approach for interpreting genome-wide expression profiles. *Proceedings of the National Academy of Sciences of the United States of America*, 102(43):15545–50, 2005.

- [33] Cole Trapnell, Brian A Williams, Geo Pertea, Ali Mortazavi, Gordon Kwan, Marijke J van Baren, Steven L Salzberg, Barbara J Wold, and Lior Pachter. Transcript assembly and quantification by RNA-Seq reveals unannotated transcripts and isoform switching during cell differentiation. *Nature biotechnology*, 28(5):511–515, 2010.
- [34] Zhong Wang, Mark Gerstein, and Michael Snyder. RNA-Seq : a revolutionary tool for transcriptomics. *Nature reviews. Genetics*, 10(1):57–63, 2010.
- [35] Jin Xiong. *Essential Bioinformatics*. 2006.

# List of Figures

1	Toluene degradation pathway . . . . .	7
2	<i>Cladophialophora immunda</i> . . . . .	8
3	Toluene and CO <sub>2</sub> values for <i>C. immunda</i> . . . . .	9
4	Directed acyclic graph (DAG) . . . . .	12
5	Approach of software <i>featureCounts</i> . . . . .	17
6	Steps of differential expression analysis . . . . .	18
7	Genome Annotation Workflow . . . . .	22
8	Correlation analysis . . . . .	29
9	GO terms for up-regulated genes . . . . .	31
10	GO terms for down-regulated genes . . . . .	33
11	KEGG pathway of TCA cycle . . . . .	35
12	Toluene degradation pathway . . . . .	38

# List of Tables

1	Hartmans'mineral media . . . . .	14
2	RNA Sequencing Read Summary . . . . .	27
3	10 most Up-regulated genes . . . . .	28
4	10 most Down-regulated genes . . . . .	28
5	Overrepresented GO terms for the genes up-regulated . . . . .	30
6	Overrepresented GO terms for the genes down-regulated . . . . .	32
7	Overrepresented KEGG pathways for the genes down-regulated . .	34
8	Enzymes of toluene degradation . . . . .	37